Performance of Mn²⁺-modified Bentonite Clay for the Removal of Fluoride from Aqueous Solution

Rabelani Mudzielwana[a] §, **Mugera W. Gitari**[a,*], **Segun A. Akinyemi**[a] and

Titus A.M. Msagati[b]

[a]*Environmental Remediation and Water Pollution Chemistry Research Group, Department of Ecology and Resources Management, School of Environmental Sciences, University of Venda, Private bag X5050, Thohoyandou, 0950, Limpopo, South Africa.*

[b]*University of South Africa, College of Science Engineering and Technology, The Science Campus, Florida Park, Roodepoort, Private Bag X6, Florida, 1710, Johannesburg, South Africa.*

ABSTRACT

A low-cost adsorbent produced from Mn²⁺-modified bentonite clay was evaluated for groundwater defluoridation. Batch experiments were used to evaluate the effect of contact time at various adsorbent dosages, adsorption isotherms and the effect of pH on fluoride removal. The results showed that the optimum F⁻ uptake occurred within the first 30 min contact time and the percentage removal increased with increasing adsorbent dosage. The data fitted better to pseudo-second-order reaction indicating that F⁻ adsorption occurred *via* chemisorption. The Weber-Morris model of intra-particle diffusion revealed that both surface and intra-particle diffusion processes were involved during the F⁻ adsorption process. Furthermore, the batch results showed that pH of the solution governed the percentage of fluoride removal with the optimum of 75.2 % fluoride removal achieved at pH 4. The adsorbent chemical stability assessment showed that chemical species were leached at trace concentrations which are within the South African National Standards (SANS) limits. Electrostatic attraction and ion-exchange were established as the major mechanisms responsible for fluoride adsorption at acidic pH and at moderate to alkaline pH levels, respectively. The study demonstrated that Mn²⁺ intercalated bentonite clay has potential for application in defluoridation of groundwater.

KEYWORDS

Adsorption, defluoridation, ion exchange, ligand exchange, intra-particle diffusion.

1. Introduction

The presence of fluoride in water has both beneficial and detrimental implications on human health depending on concentrations. At concentrations below 1 mg L⁻¹ fluoride helps in prevention of dental caries and development of bones particularly for children below the age of 10.[1,2] Conversely, at concentrations above the World Health Organization (WHO) permissible limit of 1.5 mg L⁻¹ fluoride is linked to dental and skeletal fluorosis.[3] Fluorosis is an incurable disease and it is now regarded as a global health problem with countries such as India, China, Mexico, Pakistan, Ethiopia and Egypt largely affected.[4,5]

Defluoridation is the viable option for areas that have groundwater containing fluoride concentration greater than World Health Organization standard of 1.5 mg L⁻¹.[3] Several authors have identified adsorption as suitable method for defluoridation in rural areas because it uses materials that are available at little or no cost and it is easy to operate.[6,7] Furthermore, adsorption has proved to be the sustainable method since it uses materials that can be regenerated. Some authors have also identified number of promising adsorbent including acid-activated kaolinite clay soils,[8] La³⁺-modified bentonite,[9] organosmectite,[10] smectite-rich clay soils,[11] Al/Fe oxide-coated diatomaceous earth,[12] mixed Mukondeni clay soils,[13] and MnO₂-coated bentonite clay.[14]

Clay minerals are promising materials for defluoridation of groundwater due to their abundance and cost-effectiveness. Nonetheless, clays have good adsorptive properties such as: larger chemically active surface area, higher cation exchange capacity as well as chemical and mechanical stability. Bentonite clay belongs to the class of alumino-silicates. It has a permanent negative charge caused by the isomorphous substitution of Al^{3+} for Si^{4+} in the tetrahedral layer and Mg^{2+} for Al^{3+} in the octahedral layer.[15] The negatively charged surface allows bentonite to weakly adsorb anionic pollutants. This is due to repulsion forces between the anions and the permanent negative charge on the edge of the bentonite sheet. The clay can be modified to improve its binding capacity for the anions. Bentonite clay modified with Mg^{2+}, Fe^{3+} and Al^{3+} have been observed to provide improved fluoride adsorption capacity.[16–18] Mn^{2+} is a high charge density polycation that is stable at extreme pH levels and its use in defluoridation has not been exploited. This study aimed at evaluating the applicability of Mn^{2+}-modified bentonite clay in defluoridation of groundwater. Physicochemical properties of the raw and modified bentonite clay were also evaluated. The adsorption data were modelled through the pseudo-reaction kinetics models, intra-particle diffusion model and Langmuir adsorption isotherm model. The chemical stability of the adsorbent was also evaluated.

2. Experimental

2.1. Sample Preparation

Raw bentonite clay with a chemical composition of: SiO_2 (65.2 %), Al_2O_3 (15.30 %), CaO (1.50 %), Fe_2O_3 (3.41 %), K_2O (0.98 %), MgO (3.20 %), MnO (0.1 %) and Na_2O (2.12 %) was collected from ECCA Pty. (Ltd.) in Cape Town, South Africa. All reagents and Total Ionic Solution Buffer (TISAB-III) were

purchased from Rochelle Chemicals & Lab. Equipment CC, South Africa Ltd. and they were of analytical grade. A stock solution of 1000 mg L^{-1} fluoride was prepared by dissolving 2.21 g NaF in 1 L of Milli-Q water (18.2 Ω cm^{-1}) while Mn^{2+} stock solution containing 1000 mg L^{-1} was prepared by dissolving 2.29 g MnCl$_2$ in 1 L. Working solutions for batch experiments were prepared by appropriate dilutions.

2.2. Synthesis of Mn^{2+} Bentonite Clay

Raw bentonite clay was soaked in Milli-Q water at a ratio of 1:5 in a 1000 mL beaker, the mixture was stirred for 5 min and the procedure was repeated twice. Samples were then dried in an oven for 12 h at 110 °C and then milled to pass through <250 μm sieve. To synthesize Mn^{2+}-modified bentonite, 200 mL of 50 mg L^{-1} Mn^{2+} solution was mixed with 8 g of raw bentonite in 1 L Erlenmeyer flask, the pH of the mixture was then adjusted to 8 using 0.1 M NaOH and 0.1 M HCl. The mixture was agitated for 60 min at 250 rpm on a Stuart reciprocating table shaker (SSL2, UK) and filtered through 0.45 μm filter membrane. The solid residues were dried for 12 h. at 110 °C in the oven. The modified clay was then milled to pass through <250 μm sieve. The experiments were repeated five times to generate enough Mn^{2+}-modified bentonite for subsequent experiments.

2.3. Physicochemical and Mineralogical Characterization of Mn^{2+}-modified Bentonite

The mineralogical composition of Mn^{2+} bentonite clay was examined using D8 advance X-ray diffractometer (XRD) (Bruker, Germany) and Cu–Kα radiation source. The pore size distribution, pore volume, and pore diameter were determined by Barrett Joyner Halenda (BJH) sorption model using a specific surface area analyzer (Autosorb-iQ & Quadrasorb SI, USA). Nitrogen adsorption-desorption isotherms were used to determine specific surface area of the adsorbent according to Brunauer Emmett Teller (BET) model. Cation exchange capacity was determined using ammonium acetate buffer at pH 5.4 and 7.4 as described by Gitari *et al.*[17] The surface charge and point of zero charge was determined using solid addition method as described by Kumar *et al.*[19]

2.4. Batch Defluoridation Experiments

Batch experiments were conducted to examine the effect of contact time at various adsorbent dosages, the effect of pH and leaching of chemical species from the adsorbent during adsorption of F$^-$. The effect of contact time was evaluated by varying contact time from 5 to 270 min at 0.1, 0.3 and 0.5 g 100 mL^{-1} adsor-

bent dosage. To evaluate the adsorption isotherms at various contact times, initial concentration was varied from 3 to 25 mg L^{-1}, 1 g 100 mg^{-1} adsorbent dosage was used. To evaluate the effect of pH, initial pH of the F$^-$ solution was adjusted from 4 to 12 using 0.1 M NaOH and 0.1 M HCl. The metal leaching and chemical stability assessment of the adsorbent was conducted by analyzing concentration of metals in the filtrates obtained from effect of pH experiment using Inductively Coupled Plasma-Mass Spectrometer (Agilent 7900 ICP-MS, US). All mixtures were agitated for 30 min except for the effect of contact time. After agitation samples were filtered through 0.45 μm pore membrane. The residual fluoride concentration in the treated samples was measured using an ion selective electrode 9609 BNWP Orion (USA) attached to Thermo Scientific Orion Star ISE/pH/EC meter. Similar meter was used to measure the pH. For residual fluoride, ion selective electrode was calibrated with four standards containing 1 mL of TISAB III per 10 mL of solution. The same ratio was maintained for the sample. All experiments were conducted in triplicate for better accuracy and the mean values were reported. Equations 1 and 2 were used to calculate the percentage removal and adsorption capacity, respectively.[13]

$$\% \text{ removal} = \left(\frac{C_o - C_e}{C_o} \right) \times 100 \qquad (1)$$

where C$_o$ is initial fluoride ion concentration and C$_e$ is equilibrium fluoride ion concentration.

$$Q = \left(\frac{C_o - C_e}{m} \right) \times v \qquad (2)$$

where Q = adsorption capacity (mg g^{-1}), C$_o$ = initial F$^-$ concentration (mg L^{-1}), C$_e$ = F$^-$ concentrations at equilibrium (mg L^{-1}), V = volume of solution (L) and m = mass of the adsorbent (g).

3. Results and Discussion

3.1. Physicochemical and Mineralogical Characterization

3.1.1. *Mineralogical Composition*

Figure 1 present the XRD spectra of raw and Mn^{2+}-modified bentonite clay. No significant change was observed in the XRD spectra of the bentonite after modification. However, a slight decrease in the montmorillonite peak was observed. Quantitative XRD analysis results indicated montmorillonite (i.e. 70.24 %) and quartz (i.e. 21.24 %) as the major minerals. Nevertheless, muscovite (i.e. 2.0 %) which belongs to the mica group of mineral
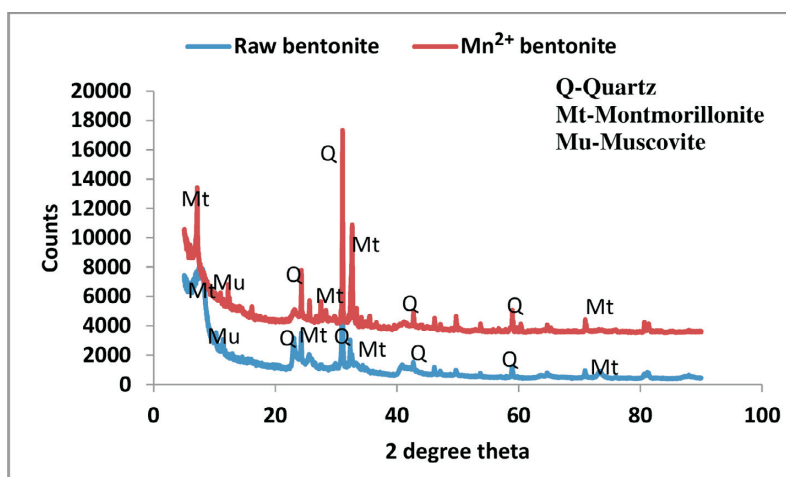

Figure 1 X-ray diffraction spectra for raw and Mn^{2+}-modified bentonite clay.

occurred in minor quantities in the bentonite clay. However, after modification, the quantities of montmorillonite and quartz decreased from 70.24 to 66.34 % and 21.24 to 17.32 %, respectively. While muscovite increased from 2.0 to 4.75 %. The decrease could be attributed to the exchange of Mg^{2+}, Na^+, K^+ and Ca^{2+} cations for Mn^{2+} ions during modification.

3.1.2. *Cation Exchange Capacity (CEC)*

The results of CEC are presented in Table 1. Cation exchange capacity for raw bentonite was found to be higher than the CEC of Mn^{2+}-modified bentonite. pH of the buffering media does not seem to have significant influence on the exchangeable cation concentration and CEC. Similar results on CEC have been reported by Gitari *et al.*[17]

3.1.3. *Determination of pHpzc*

Figure 2 presents the pHpzc of raw bentonite (a) and Mn^{2+}-modified bentonite (b). The pHpzc values for raw bentonite and Mn^{2+} bentonite were found to be 8.4 and 8.8, respectively. At pH above the pHpzc the clay surface is negatively charged while at pH below pHpzc the clay surface is positively charged. Both raw and Mn^{2+}-modified bentonite clay have high pHpzc

indicative of clay dominated by alumino-silicate materials and manganese oxides. Modification of the raw bentonite clay with Mn^{2+} increases the pHpzc and which extends the pH range for adsorption of anions. This trend indicated that the Mn^{2+}-modified bentonite clay will have high adsorption capacity for anions than the raw bentonite clay. An increase in pHpzc of bentonite clay after modification has also been reported for Al^{3+}-modified bentonite by Masindi *et al.*[16]

3.1.4. *Surface Properties Analysis*

Surface properties of raw bentonite and Mn^{2+}-modified bentonite are presented in Table 1. The results showed an increase in total surface area of the bentonite after modification from 43.48 to 66.41 $m^2 g^{-1}$. Furthermore, pore volume decreased to 0.09 $cm^3 g^{-1}$ (Table 1). This could be attributed to swelling or hydration of the bentonite clay during intercalation of Mn^{2+} ions. The average pore diameter of raw bentonite is relatively higher when compared to that of Mn^{2+}-modified bentonite clay (Table 1). This suggests that Mn^{2+} ions were incorporated onto the surface of the raw clay, including adsorption on the edges. Figure 3 depicts pore distribution curve of raw and Mn^{2+}-modified bentonite. It is observed that majority of the pores lies within 2 nm and 50 nm indicating that both raw and Mn^{2+}-modified bentonite are mesoporous in nature.

3.2. Batch Experiments

3.2.1. *Effect of Contact Time and Adsorption Kinetics*

Figure 4 depicts the relationship between contact time and percentage F^- removal. It is evident that F^- removal was rapid during the first 30 min of the experiment where optimum uptake of F^- was achieved. Thereafter, slight change in the percentage F^- removal was observed which indicate that the adsorbent was
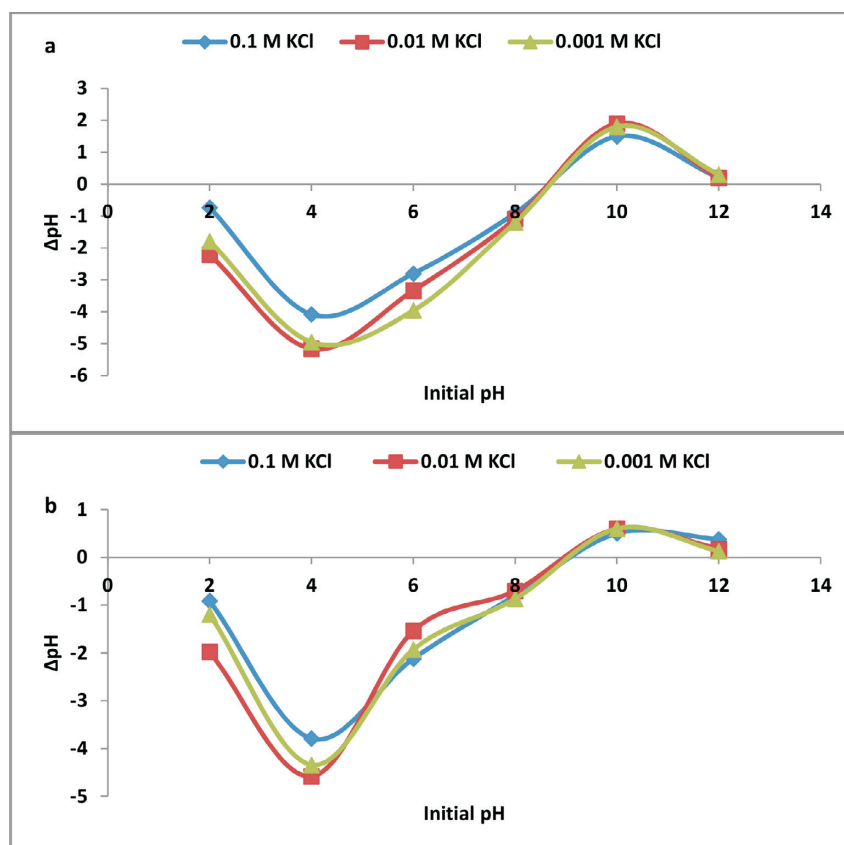
Table 1 Cation exchange and surface properties of raw and Mn^{2+}-modified bentonite clay.

Parameter	Raw bentonite	Mn^{2+}-modified bentonite
CEC pH 5.4	288	111
pH 7.4	294	114
Surface area /$m^2 g^{-1}$	43.48	66.41
Pore volume /$cm^3 g^{-1}$	0.088	0.09
Pore diameter /nm	7.9	5.5

Figure 2 pH$_{pzc}$ of raw bentonite clay (**a**) and Mn^{2+}-modified bentonite clay (**b**).
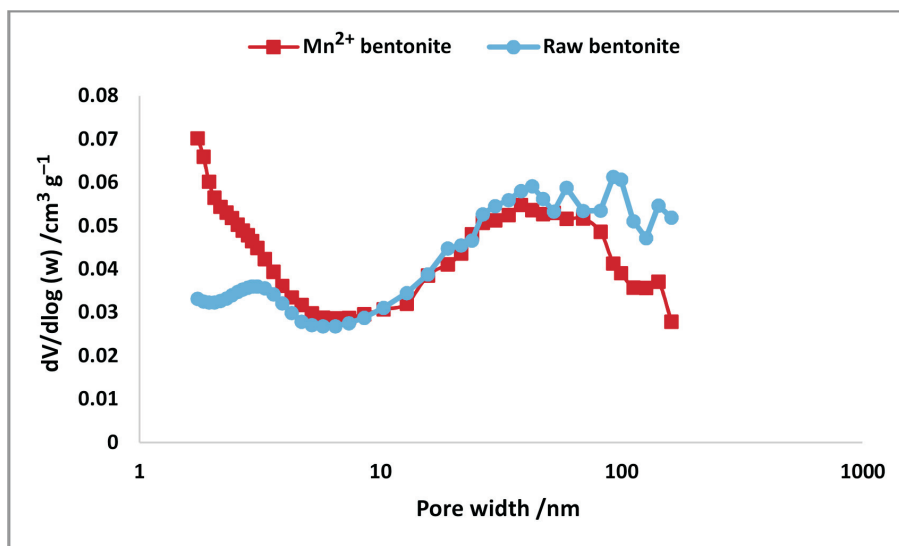
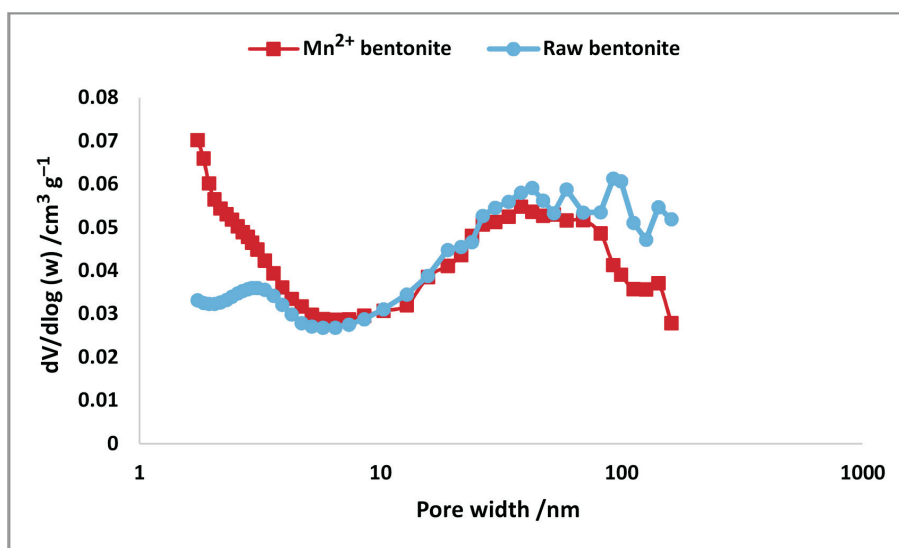**Figure 3** Pore distribution of raw and Mn^{2+}-modified bentonite clay.

Figure 4 Variation of % F$^-$ removal as a function of contact time for various adsorbent dosages (3 mg L^{-1} F$^-$, pH 5.54 ± 0.5 and 250 rpm shaking speed, n = 3).

getting saturated and system has reached equilibrium. The increase in F$^-$ removal is attributed to the availability of sorption sites in the adsorbent. The similar trend was observed at both adsorbent dosages and the percentage F$^-$ removal was increasing with adsorbent dosage. Contact time of 30 min was taken as the optimum time and was applied in subsequent experiments.

Pseudo-first and second-order reaction based models were employed to determine the rate limiting steps of fluoride adsorption onto Mn^{2+}-modified bentonite as well as the potential rate controlling steps. The pseudo first order is shown in the Equation 3 and it is used to describe liquid–solid phase adsorption systems, and it is the earliest known kinetic model describing the adsorption rate based on the adsorption capacity.[20]

$$\log(q_e - q_t) = \log(q_e - \frac{k_{ad}t}{2.303} \quad (3)$$

Pseudo second order is shown in the linear Equation 4 and it is used to describe chemisorption, as well as cation exchange reactions.[14]

$$\frac{t}{q_t} = \frac{1}{K_{2ads}q_e^2} + \frac{1}{q_e}t \quad (4)$$

where q$_e$ and q$_t$ (both in mg g^{-1}) are the amount adsorbed per unit mass at a time, t (in min). K$_{ad}$ and K$_{2ads}$ are first- and second-order rate constant (g mg^{-1} min^{-1}). The value of K$_{ad}$ is determined from the slope and intercepts of log (q$_e$ – q$_t$) *vs.* t (min) and the value of K$_{2ads}$ is determined from the slope and intercepts of t/q$_t$ *vs.* q$_e$. Adsorption of fluoride ion onto Mn^{2+} bentonite did not follow the pseudo-first-order process since it did not yield a straight line (figure no presented). Figure 5 shows the plot of t/q with time which indicate high correlation coefficient at both adsorbent doses. This implies that fluoride sorption onto Mn^{2+}-modified bentonite clay followed pseudo second order and is chemisorption. The constant values of pseudo first and second order are presented in Table 2.

During the process of fluoride adsorption, fluoride ions also diffuses into the interior of the adsorbent. Intra-particle diffusion model based on the hypothesis proposed by Weber Morris was tested to identify the diffusion mechanism.[21] The linear equation of the intra-particle diffusion is given by the Equation 5 below.
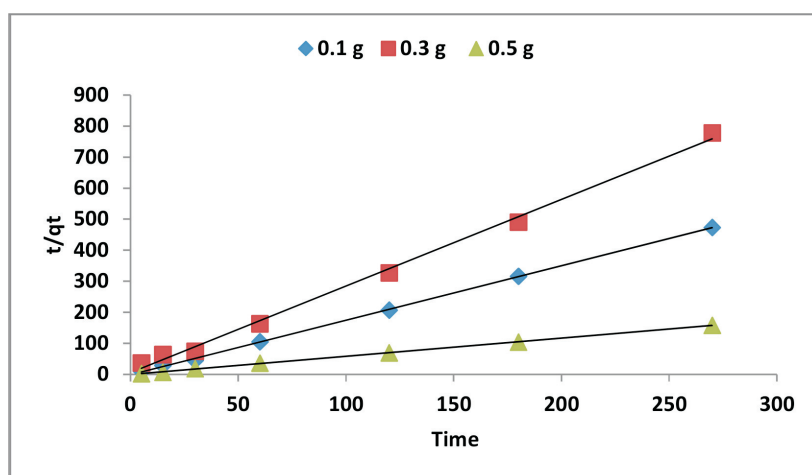
$$q_t = K_i \sqrt{t} \quad (5)$$

Figure 5 Pseudo-second-order plot at various adsorbent doses (3 mg L^{-1} F$^-$, pH 5.54 and shaking speed of 250 rpm).

where q_t is the amount adsorbed (mg g^{-1}) at a given time t (min), K_i (mg g^{-1} min^{-1}) is the intra particle diffusion rate constant and it is determined from the slope of $t^{0.5}$ *vs.* q_t.

This indicates that if the plot of q_t against $t^{0.5}$ gives straight line passing through the origin, then the adsorption is solely controlled by intra-particle diffusion, while a bilinear plot indicates that adsorption occurred *via* film and intra-particle diffusion mechanism.[1]

Figure 6 shows the plot of intra-particle diffusion model. Adsorption of fluoride onto Mn^{2+} bentonite showed bilinear plot with the initial plot (phase 1) indicating external diffusion and the second plot (Phase 2) indicates intra-particle diffusion. The intra-particle rate constants K_{i1} and K_{i2} obtained from the plot are shown in Table 3. At both adsorbent dosages, K_{i1} value is greater than the K_{i2} value, indicating that the initial step is faster than the final step where equilibrium was established. Furthermore, the K_{i1} value increases with increasing adsorbent dosage. This could be attributed to difference in the rate of mass transfer in the initial and final stages of adsorption. This observed trend is connected to a mechanism consisting of an external mass transfer followed by diffusion into micro- and mesoporous surfaces. In conclusion, fluoride adsorption onto Mn^{2+}-modified bentonite is a complex process involving external and internal diffusion of F$^-$ ions.

3.2.2. *Adsorption Isotherms*

Figure 7 shows the effect of adsorbate concentration on the percentage fluoride removal at various contact times. It is

Table 2 Pseudo-first and second-order kinetics constant values

	Pseudo first order		Pseudo second order		
	K_{ad} /min^{-1}	R^2	q_e /mg g^{-1}	K_{2a} /g mg^{-1} min^{-1}	R^2
0.1 g 100 mL^{-1}	2.1 ×10^{-2}	0.47	0.56	2.73	0.99
0.3 g 100 mL^{-1}	5.1 × 10^{-3}	0.35	0.33	1.36	0.99
0.5 g 100 mL^{-1}	4.6 ×10^{-3}	0.05	2.4	0.52	0.99

observed that the percentage F$^-$ removal decreased with an increase in the initial concentration. Similar trend was observed at all the contact times. This could be due to availability of more fluoride ions in the solution at higher adsorbate concentration. Besides, it could also indicate that fluoride binding sites of the adsorbent was getting exhausted.

Langmuir isotherm was used to describe the data (Langmuir; 1997). It is applicable to homogeneous adsorption where adsorption process has equal activation energy. It is assumed that the

Table 3 Intra-particle diffusion constant values

Absorbent dosages	Constant values	
	K_{i1}	K_{i2}
0.1 g 100 mL^{-1}	0.016	-3×10^{-5}
0.3 g 100 mL^{-1}	0.022	-0.2×10^{-5}
0.5 g 100 mL^{-1}	0.13	-8×10^{-8}

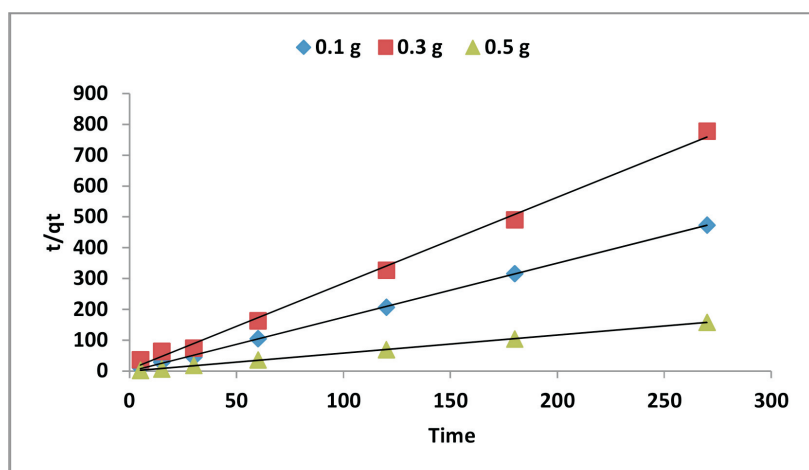**Figure 6** Plot of intra-particle diffusion at various adsorbent dosages (3 mg L^{-1} F$^-$, pH 5.54 and shaking speed of 250 rpm, n = 3).

adsorbent surface is uniform, i.e. all the adsorption sites are equivalent and adsorption molecules do not interact (Zhang *et al.* 2011; Gosh *et al.* 2015). The linear equation for Langmuir isotherm model is expressed in the Equation 6:

$$\frac{C_e}{Q_e} = \frac{1}{Q_m b} + \frac{C_e}{Q_m} \tag{6}$$

where, C_e is the equilibrium concentration (mg L^{-1}). Q_e is the adsorption capacity (mg L^{-1}). Q_m is theoretical maximum adsorption capacity (mg g^{-1}). b is the Langmuir constant related to enthalpy of adsorption (L mg^{-1}). Q_m and b are determined from the slope and intercept of the plot of $\frac{C_e}{Q_e}$ *vs.* C_e. Calculated Langmuir constants are presented in Table 4 and the Langmuir plots are shown in Fig. 8.

Furthermore, to reveal the feasibility of Langmuir adsorption isotherm, the dimensionless parameter of the equilibrium or adsorption intensity (R_L) was used for further analysis of Langmuir equation. The values of R_L were calculated using Equation 7:

$$R_L = \frac{1}{1 + bC_o} \tag{7}$$

where C_o is the initial concentration (mg L^{-1}) and b is the Langmuir constant (L mg^{-1}).

Table 4 Constant values for Langmuir isotherm.

	q_m /mg g^{-1}	b /L mg^{-1}	R^2
30 min	2.21	0.88	0.99
60 min	2.22	0.55	0.96
120 min	2.40	0.10	0.87

The value of R_L less than 1 generally indicate favourable adsorption while greater than 1 indicate unfavourable adsorption. Figure 9 shows calculated R_L values which ranged between 0 and 1 indicating adsorption process was favourable at room temperature for all the adsorbate concentrations tested.

3.2.3. *Effect of pH and Fluoride Removal Mechanism*

Figure 10 shows the effect of initial pH on percentage fluoride removal. The removal of F$^-$ removal decreases from 75.2 to 24.33 % at pH 4 and pH 6, respectively. Thereafter, the F$^-$ removal increased to 30 % at pH 10 and this was followed by significant decrease at pH greater than 10. This observed trend could be due to the abundance of OH$^-$ ions in alkaline pH that compete with F$^-$ for adsorption sites. The equilibrium pH at initial pH of 4 was found to be 8.96 which is suitable for human consumption. The pHpzc of the Mn^{2+}-modified bentonite was found to be at pH 8.8. Therefore, at pH <8.8 the surface of the clay will be
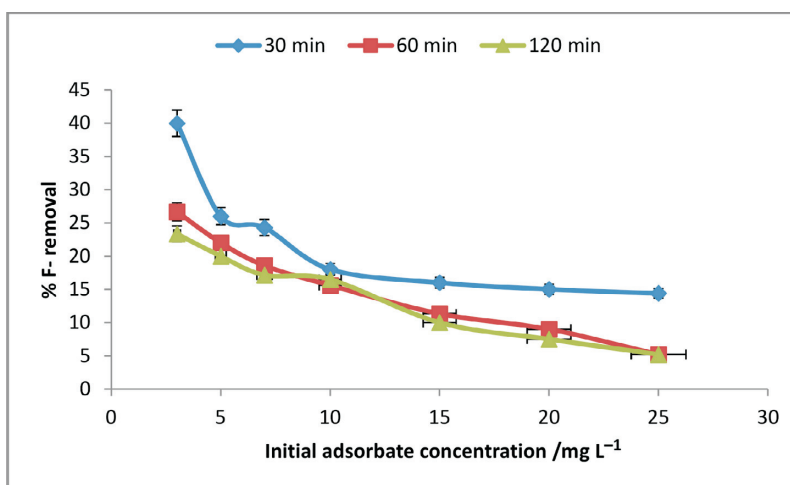

Figure 7 Variation of % F$^-$ removal by Mn^{2+} bentonite clay as a function of adsorbate concentration at various contact times (adsorbent dosage 1.0 g 100 mL^{-1}, pH of 5.24 and shaking speed of 250 rpm).
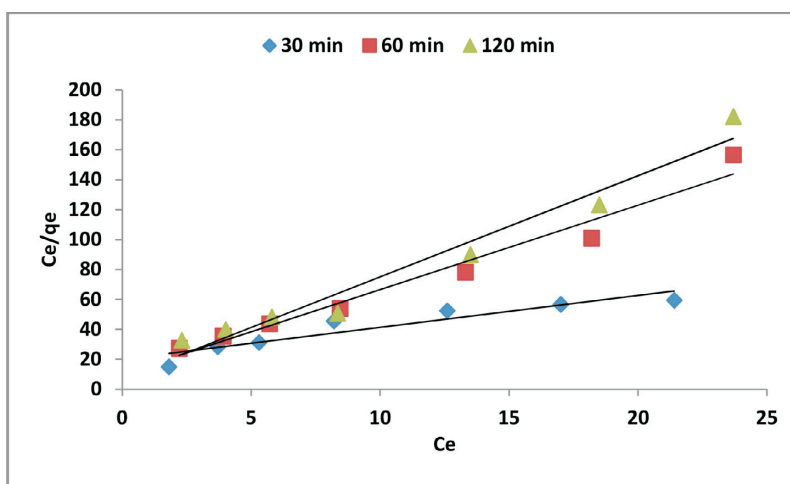

Figure 8 Langmuir isotherm plot for fluoride removal onto Mn^{2+} incorporated bentonite clay at 30, 60 and 120 min contact time (250 rpm shaking speed, pH 5.54 ± 0.5 and adsorbent dosage of 1 g 100 mL^{-1}).
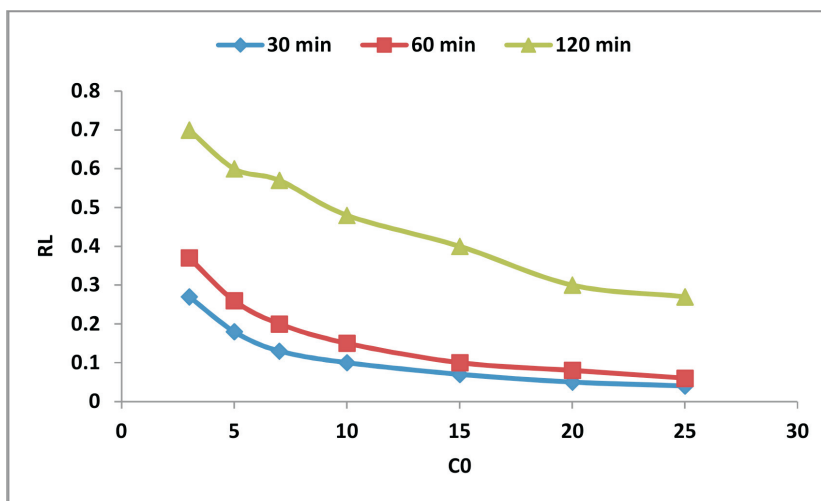
Figure 9 R_L values for adsorption of F⁻ onto Mn²⁺ intercalated bentonite clay.

positively charged (Equation 8) and at pH > 8.8 the surface of the adsorbent will be negatively charged. At pH less than the pHpzc, fluoride was removed through electrostatic attraction mechanism (Equations 9 & 10), whereas at moderate pH, fluoride adsorption occurs through ion exchange (Equation 11). At pH higher than the pHpzc where the surface of the clay is negatively charged fluoride adsorption also occurs through ion exchange mechanism (Equation 12).

$$\equiv M(OH) + H^+ \Leftrightarrow \equiv MOH_2^+ \tag{8}$$

$$\equiv MOH + H_3O^+ + F^- \Leftrightarrow \equiv MOH_2^+ - F^- + H_2O \tag{9}$$

$$\equiv MOH + H_2O + F^- \Leftrightarrow \equiv MOH_2^+ - F^- + OH^- \tag{10}$$

$$\equiv MOH + F^- \Leftrightarrow MF + OH^- \tag{11}$$

$$\equiv M(OH)_2^- + 2F^- \Leftrightarrow MF_2 + 2OH^- \tag{12}$$

where ≡ M represent metal in the adsorbent surface (Mn, Si and Al)

3.3. Leaching Assessment of the Mn²⁺-modified Bentonite

Concentrations of chemical species leached are shown in Fig. 11a,b. From the results, it is observed that the concentration of Na⁺ was very high at both pH levels. This could be attributed to the use of NaOH for pH adjustment. High Si⁴⁺ and Al³⁺ concentration was observed at higher pH levels. This observed

trend could have been influenced by chemical dissolution of silica at higher pH. Metals such as Mn²⁺, Fe²⁺, Al³⁺ and Cu²⁺ were released at minor concentrations and were found to be within the SANS permissible limits.[20] The final F⁻ concentration in the solution at pH 4, 6, 8, 10 and 12 were found to be 1.26, 2.27, 2.19, 2.12 and 3.95 mg L⁻¹, respectively. Table 5 shows the comparison between concentration of metal species in treated water and the SANS-241 permissible limits. Therefore, based on the obtained data, Mn²⁺-modified bentonite is a promising material for defluoridation of groundwater since it does not give rise to secondary pollutants in the treated water.

3.4. Comparison with Other Adsorbent

Table 6 present the comparison of the adsorption capacities between Mn²⁺-modified bentonite and other poly-cation-modified bentonite reported in the literature. Mn²⁺-modified bentonite reported in this study showed higher adsorption capacity compared to Mg²⁺ and La²⁺-modified bentonite. Unlike Fe³⁺ and Al³⁺-modified bentonite clays which exhibited highest adsorption capacity at pH 2, Mn²⁺ bentonite exhibited its maximum adsorption capacity at initial pH 4.

4. Conclusions

The physicochemical properties and fluoride removal efficiency of Mn²⁺-modified bentonite were successfully evaluated.
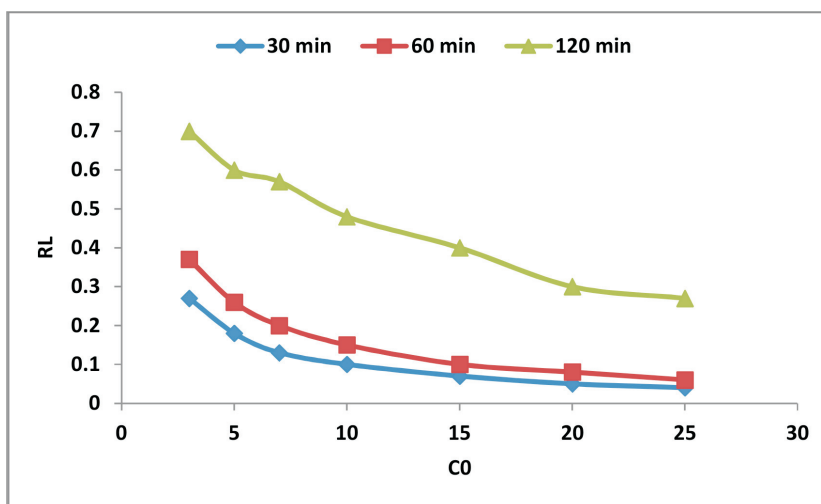

Figure 10 Variation of % F⁻ removal and equilibrium pH during F⁻ adsorption onto Mn²⁺ bentonite clay as a function of pH during (contact time 30 min, adsorbent dosage 1.0 g 100 mL⁻¹, 5 mg L⁻¹ F⁻ and shaking speed of 250 rpm, n = 3)

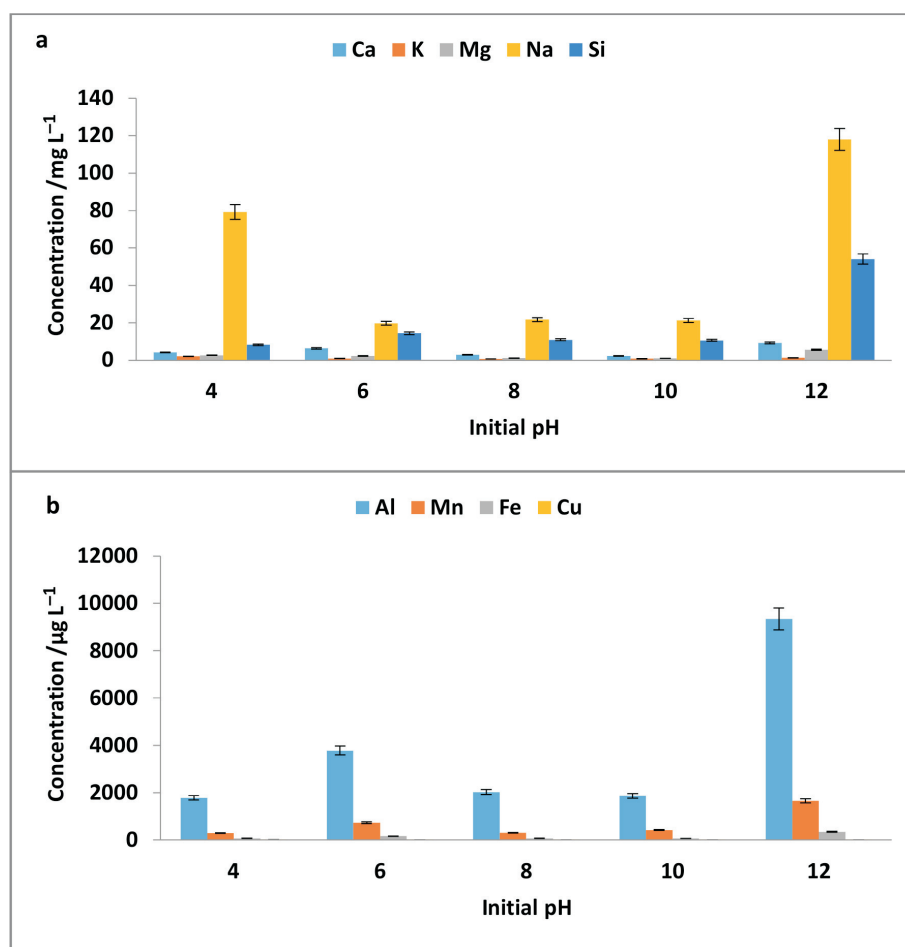**Figure 11** Concentration of chemical species in treated water at various pH. (**a**) in mg L^{-1}, and (**b**) in μg L^{-1} (n = 3).

Table 5 Comparison of species concentration at various pH with SANS-241 guideline values for chemical species.

	pH 4	pH 6	pH 8	pH 10	pH 12	SANS-241 /mg L^{-1}
Ca /mg L^{-1}	4.15 ± 0.05	6.3 ± 0.05	2.87 ± 0.01	2.25 ± 0.01	9.23 ± 0.01	0–32
K /mg L^{-1}	2.04 ± 0.01	0.93 ± 0.01	0.73 ± 0.05	0.79 ± 0.01	1.3 ± 0.01	0–50
Mg /mg L^{-1}	2.6 ± 0.05	2.25 ± 0.05	1.109 ± 0.01	1.023 ± 0.01	5.648 ± 0.05	0–30
Na /mg L^{-1}	79.2 ± 0.01	19.7 ± 0.01	21.61 ± 0.01	21.23 ± 0.01	118 ± 0.01	0–100
Si /mg L^{-1}	8.2 ± 0.01	14.36 ± 0.01	10.9 ± 0.01	10.6 ± 0.05	54.08 ± 0.05	–
Al /mg L^{-1}	0.101 ± 0.05	3781.54 ± 0.5	2028.43 ± 0.01	1864.429 ± 0.02	9341.13 ± 0.1	0–0.15
Mn /mg L^{-1}	0.029 ± 0.01	735.82 ± 0.05	308.02 ± 0.05	419.83 ± 0.01	1655.48 ± 0.01	0–0.05
Fe /mg L^{-1}	0.008 ± 0.5	167.73 ± 0.01	81.5 ± 0.01	69.63 ± 0.01	345.99 ± 0.01	0–0.1
Cu /mg L^{-1}	0.0012 ± 0.01	6.38 ± 0.01	3.18 ± 0.01	2.31 ± 0.01	3.78 ± 0.01	0–1

n = 3

The mineralogical characterization results by XRD showed that modification of bentonite clay by Mn^{2+} polycations does not alter the parent mineralogy of the clay. However, it decreases the content of the major minerals. The modified bentonite showed higher surface area and pHpzc compared to the raw bentonite clay. Conversely, the CEC decreased after modification by Mn^{2+}. A maximum of 75.2 % F^- removal was achieved from the initial 5 mg L^{-1} using 1 g 100 mL^{-1} adsorbent dosage at a contact time of

Table 6 Comparison of Mn^{2+}-modified bentonite and other reported adsorbents.

Adsorbent	q_e /mg g^{-1}	Experimental conditions	Reference
Mg^{2+} bentonite	2.26	pH 2–10; 5 mg L^{-1} F^-	Thakre *et al.*[16]
Fe^{3+} bentonite	2.91	pH 2; 10 mg L^{-1} F^-	Gitari *et al.*[17]
Al^{3+} bentonite	5.7	pH 2; 20 mg L^{-1} F^-	Masindi *et al.*[18]
La^{3+} bentonite/Chitosan beads composite	2.31	pH 5; 10 mg L^{-1} F^-	Yi *et al.*[23]
Mn^{2+} bentonite	2.4	pH 4; 5 mg L^{-1} F^-	Present study

30 min and initial pH of 4. The adsorption data fitted better to pseudo-second-order reaction kinetics model indicating that F$^-$ adsorption occurred *via* chemisorption. Langmuir isotherm model described the data successfully indicating that adsorption occurred in a monolayer surface. Fluoride adsorption onto Mn^{2+} bentonite occurred through electrostatic attraction and ion exchange adsorption mechanism at lower and higher pH levels, respectively. Leaching assessment showed that the released chemical species from the adsorbent at various pH levels fall within SANS-241 permissible limits. The results proved that Mn^{2+} bentonite has the potential for use in fluoride removal in areas where groundwater has maximum fluoride concentration of 3 mg L^{-1}.

§ORCID iDs

R. Mudzielwana: orcid.org/0000-0002-7744-4561
M.W. Gitari: orcid.org/0000-0002-6387-0682

References

1 N. Chen, Z. Zhang, C. Feng, M. Li, D. Zhu and N. Sugiura, Studies on fluoride adsorption of iron-impregnated granular ceramics from aqueous solution, *J. Mater. Chem. Phys.*, 2011, **125**, 293–298.

2 T. Nur, P. Loganathan, T.C. Nguyen, S. Vigneswaran, G. Singh and J. Kandasamy, Batch and column adsorption and desorption of fluoride using hydrous ferric oxide: solution chemistry and modelling, *J. Chem. Eng.*, 2014, **247**, 93–102.

3 World Health Organization, *Guidelines for Drinking-water Quality*, 4th edn., Geneva, Switzerland, 2011.

4 S.V. Jadhav, E. Bringas, G.D. Yadav, V.K. Rathod, I. Ortiz and K.V. Marathe, Arsenic and fluoride contaminated groundwaters: a review of current technologies for contaminants removal, *J. Environ. Manage.*, 2015, **162**, 306–325.

5 K.M. Kut, A. Sarswat, A. Srivastava, C.U. Pittman, U. Mohan, A review of fluoride in African groundwater and local remediation methods, *Groundw. Sust. Dev.*, 2016, **2**, 190–212.

6 R. Tovar-Gómez, M.R. Moreno-Virgen, J.A. Dena-Aguilar, V. Hernández-Montoya, A. Bonilla-Petriciolet and M.S. Montes-Morán, Modeling of fixed-bed adsorption of fluoride on bone char using a hybrid neural network approach, *Chem., Eng.*, 2013, **228**, 1098–1109.

7 Y. Yu, L. Yu and J.P. Chen, Adsorption of fluoride by Fe–Mg–La triple-metal composite: adsorbent preparation, illustration of performance and study of mechanisms, *Chem. Eng.*, 2015, **262**, 839–846.

8 P.K. Gogoi and R. Baruah, Fluoride removal from water by adsorption on acid activated kaolinite clay, *Indian J. Chem. Technol,.* 2008, **15**, 500–503.

9 S. Kamble, P. Dixit, S.S. Rayalu and N.K. Labhsetwar, Defluoridation of drinking water using chemically modified bentonite clay, *Desal. Water Treat.*, 2009, 249, 687–693.

10 S. Gammoudi, N. Frini-Srasra, E. Srasra, Preparation, characterization of organo-smectites and fluoride ion removal, *Int. J. Miner. Process.*, 2013, **125**, 10–17.

11 R. Mudzielwana, W.M. Gitari, T.A.M. Msagati, Characterization of smectite-rich clay soil: implication for groundwater defluoridation, *S. Afr. J. Sci.*, 2016, **112** (11-12), 41–48.

12 A.A. Izuagie, W.M. Gitari and J.R. Gumbo, Synthesis and performance evaluation of Al/Fe oxide coated diatomaceous earth in groundwater defluoridation: towards fluorosis mitigation, *J. Environ. Sci. Heal. A.*, 2016, 1–15.

13 T. Ngulube, M.W. Gitari, H. Tutu, Defluoridation of groundwater using mixed Mukondeni clay soils, *WST: Water Supply*, 2017, **17**(2), 480–492.

14 R. Mudzielwana, M.W. Gitari, S.A. Akinyemi, T.A.M. Msagati. Synthesis and physicochemical characterization of MnO$_2$ coated Na-bentonite for groundwater defluoridation: adsorption modelling and mechanistic aspect, *Appl. Surf. Sci.*, 2017, **422**, 745–753.

15 Y. Ma, S.G. Wang, M. Fan, W.X. Gong and B.Y. Gao, Characteristics and defluoridation performance of granular activated carbons coated with manganese oxides, *J. Hazard. Mater.*, 2012, **168**, 1140–1146.

16 D. Thakre, S. Rayalu, R. Kawade, S. Meshram, J. Subrt and N. Labhsetwar, Magnesium incorporated Bentonite clay for defluoridation of drinking water, *J. Hazard. Mater.*, 2010, **180**, 122–130.

17 W.M. Gitari, T. Ngulube, V. Masindi and J.R. Gumbo, Defluoridation of groundwater using Fe^{3+}-modified bentonite clay: optimization of adsorption condition, *J. Desalin. Water Treat.*, 2013, 1–13.

18 V. Masindi, W.M. Gitari and T. Ngulube, Defluoridation of drinking water using Al^{3+}-modified bentonite clay: optimization of fluoride adsorption conditions, *Toxicol. Environ. Chem.*, 2014, **96**(9), 1–16.

19 E. Kumar, A. Bhatnagar, U. Kumar and M. Sillanpaa, Defluoridation from aqueous solution by nano-alumina: characterization and sorption studies, *J. Hazard. Mater.*, 2011, **186**, 1042–1049.

20 N.A. Oladoja, B. Helmreich, H.A. Bello, Towards the development of a reactive filter from green resource for groundwater defluoridation, *Chem. Eng. J.*, 2016, **301**, 166–177.

21 Y. Jia, B.S. Zhu, K.S. Zhang, Z. Jin T. Luo, X.Y. Yu, L.T. Kong. and J.H. Liu. Porous 2-line ferrihydrite/byerite composite (LFBC): fluoride removal performance and mechanism, *Chem. Eng. J.*, 2015, **268**, 325–336.

22 *South African National Standard (SANS) 241 Drinking Water Specification*, South African Bureau of Standards (SABS), Pretoria, South Africa, 2006.

23 Z. Yi, X. Ying, C. Hao, L. Bingjie, G. Xiang, W. Dongfeng and L. Peng, La (III)-loaded bentonite/chitosan beads for defluoridation from aqueous solution, *J. Rare Earth.*, 2014, **32**(5), 458–469.